

# MOUNTAIN-PLAINS CONSORTIUM

MPC 19-395 | S. Chen, L. Chen and Y. Zhou

Analytical Modeling of  
Seismic Performance of  
Curved and Skewed Bridges



A University Transportation Center sponsored by the U.S. Department of Transportation serving the Mountain-Plains Region. Consortium members:

Colorado State University  
North Dakota State University  
South Dakota State University

University of Colorado Denver  
University of Denver  
University of Utah

Utah State University  
University of Wyoming

# **Analytical Modeling of Seismic Performance of Curved and Skewed Bridges**

Suren Chen  
Luke Chen  
Yufen Zhou

Department of Civil and Environmental Engineering  
Colorado State University  
Fort Collins, Colorado

August 2019

## **Acknowledgements**

The funds for this study were provided by the United States Department of Transportation to the Mountain-Plains Consortium (MPC).

## **Disclaimer**

The contents of this report reflect the views of the authors, who are responsible for the facts and the accuracy of the information presented herein. This document is disseminated in the interest of information exchange. The report is funded, partially or entirely, by a grant from the U.S. Department of Transportation's University Transportation Centers Program. However, the U.S. Government assumes no liability for the contents or use thereof.

NDSU does not discriminate in its programs and activities on the basis of age, color, gender expression/identity, genetic information, marital status, national origin, participation in lawful off-campus activity, physical or mental disability, pregnancy, public assistance status, race, religion, sex, sexual orientation, spousal relationship to current employee, or veteran status, as applicable. Direct inquiries to Vice Provost for Title IX/ADA Coordinator, Old Main 201, NDSU Main Campus, 701-231-7708, [nodsu.eoaa.ndsu.edu](mailto:nodsu.eoaa.ndsu.edu).

## **ABSTRACT<sup>1</sup>**

Due to the current limitations on seismic forecasting, there is a high chance that a considerable number of vehicles would remain on a bridge when an earthquake occurs. In traditional seismic analyses, traffic loads were often ignored. Existing mode-based bridge-traffic interaction analysis usually cannot consider nonlinearity effects of the bridge under earthquakes, which are critical to short- and medium-span bridges. Traditional nonlinear seismic analyses using commercial or open-source software cannot directly incorporate complex dynamic interactions between moving vehicles and bridges. So far there is no reported methodology that can be used for nonlinear seismic analyses of typical short- and medium-span bridges while rationally considering the coupling effects between the bridge, moving vehicles, and earthquake simultaneously. A hybrid simulation approach is proposed to conduct the nonlinear seismic analysis of the bridge/traffic/earthquake system by integrating the stochastic traffic flow simulation, the mode-based fully-coupled simulation technique of the bridge-traffic system, and the nonlinear seismic analysis platform that was developed based on OpenSees. A skewed and curved bridge, which is a common design to overcome complex intersections and terrain restrictions for short- and medium-span bridges, is studied as a demonstration; this is followed by the numerical investigation of the bridge seismic performance and the impact of incorporating traffic loads. The results suggest the proposed hybrid methodology can capture the complex dynamic interactions between the bridge and multiple vehicles, as well as the nonlinear seismic performance to provide rational prediction results.

---

<sup>1</sup> This study has been accepted as a journal paper: Chen, L., Zhou, Y. and Chen, S. (2019). "Hybrid nonlinear seismic analysis of bridges with moving traffic," *J. of Aerospace Engineering*, ASCE (in press).

## TABLE OF CONTENTS

<b>1. INTRODUCTION AND LITERATURE REVIEW .....</b>	<b>1</b>
1.1 Background .....	1
1.2 Literature Review .....	1
1.3 Organization of This Report.....	2
<b>2. MODE-BASED BRIDGE/TRAFFIC INTERACTION ANALYSIS.....</b>	<b>3</b>
2.1 Stochastic Traffic Flow Simulation.....	3
2.2 Fully-coupled Bridg-traffic Interaction Model.....	3
<b>3. HYBRID NONLINEAR SEISMIC ANALYSIS FRAMEWORK CONSIDERING TRAFFIC IMPACT WITH OPENSEES.....</b>	<b>5</b>
3.1 Equivalent Moving Traffic Loads (EMTL).....	5
3.2 EMTL-FE Hybrid Strategy .....	5
<b>4. NUMERICAL INVESTIGATION OF PROTOTYPE BRIDGE .....</b>	<b>7</b>
4.1 Prototype bridge and scenario earthquake records.....	7
4.2 Traffic Loads from Bridge-traffic Interaction Effects.....	9
4.3 Nonlinear Seismic Analysis Results .....	11
4.4 Impact of Different Excitation Scenarios of Ground Motions .....	17
4.5 Impact of Traffic on Seismic Response .....	21
<b>5. CONCLUSION.....</b>	<b>26</b>
<b>6. REFERENCES.....</b>	<b>27</b>

## LIST OF TABLES

Table 4.1	Scenario ground motion selection.....	9
Table 4.2	Input direction and intensities of different scenarios .....	17

## LIST OF FIGURES

Figure 2.1	The numerical dynamic model for the heavy truck with one trailer .....	4
Figure 3.1	Flowchart for EMTL-FE hybrid strategy .....	6
Figure 4.1	Geometries of prototype bridge and corresponding straight counterpart.....	7
Figure 4.2	3-D OpenSees model of the prototype bridge.....	8
Figure 4.3	Scenario seismic excitation.....	9
Figure 4.4	Side view of the vehicle wheels on the traffic lanes for the prototype bridge .....	10
Figure 4.5	Longitudinal locations of the vehicles on the fast lane in the busy traffic flow.....	10
Figure 4.6	EMTL at the center location of the span on the skewed bridge deck .....	11
Figure 4.7	Longitudinal moments of individual columns .....	13
Figure 4.8	Transverse moments of individual columns .....	14
Figure 4.9	Column demand/capacity ratio for individual columns .....	15
Figure 4.10	Girder-abutment gap width between girder and abutment.....	16
Figure 4.11	Longitudinal pounding forces between girder and abutment.....	16
Figure 4.12	Transverse deformation of columns.....	18
Figure 4.13	Transverse moment comparison of columns.....	19
Figure 4.14	Deck vertical response comparison.....	20
Figure 4.15	Traffic effect to column ColL1 .....	21
Figure 4.16	Traffic effect to column ColL1 (a) axial forces (b) zoomed out view .....	22
Figure 4.17	Deck peak vertical displacements .....	23
Figure 4.18	Traffic load impact on vertical displacement and acceleration response at midspan.....	25

# **1. INTRODUCTION AND LITERATURE REVIEW**

## **1.1 Background**

As a result of the current limitations on seismic forecasts, it is very likely that normal traffic will remain on a bridge when an earthquake occurs. In traditional seismic analyses, traffic was typically ignored. Existing seismic performance predictions of short- and medium-span bridges without considering traffic impact often show that some bridge components either experience or are on the verge of severe damage from earthquakes. Therefore, as an important type of service loads, traffic impact on the bridge's seismic performance should not be ignored. More realistic seismic performance of the bridge can be critical to future bridge seismic design, prevention, and planning, especially for those with narrow safety margins.

## **1.2 Literature Review**

The current AASHTO specification defines the extreme event limit state I by introducing a “project-specific” load combination factor to superpose the bridge response result under the design traffic load to that under the seismic load (AASHTO 2012). The superposition method, despite its popularity, cannot capture the full coupling effects between seismic excitation, traffic loads, and bridge. The lack of considering bridge/vehicle coupling effects (Deng and Cai 2010; Deng et al. 2015) is especially critical for short- and medium-span bridges when nonlinear structural behavior, local damages to some bridge components and even structural collapse have been observed under earthquakes. In addition to structural integrity, ignoring the dynamic interactions between the bridge, vehicles and earthquake will also pose challenges in terms of assessing the serviceability, such as driving safety and ride comfort of vehicles on the bridge. Therefore, there still exists a gap between the reality and the current state of the art in terms of seismic analysis of short- and medium-span bridge and traffic systems, which may jeopardize the rational risk assessment of serviceability, member damage and progressive failure of the bridge during earthquakes.

In early studies related to traffic load modeling, vehicles were considered as moving forces (Timoshenko, 1974) or moving masses (Blejwas, 1979), which have been incorporated in bridge design guidelines, such as Japan Road Association codes (2002) and AASHTO LRFD Design (2012). There have been only a few studies on bridge seismic analysis considering vehicle and bridge dynamic interactions; these include numerical studies by Kamada et al. (1992) and Kim et al. (2010) with simple vehicle and bridge models. Ghosh (2013) proposed a framework of joint seismic and live-load fragility assessment of bridges, where its truck presence model assumed traffic flow in a constant speed for a representative truck. Recently, Kameshwar and Padgett (2017) studied the impacts of vehicles on bridge seismic response and fragility by assuming the vehicles were not in motion. The study covered three different types of stationary trucks and found that traffic can have a large impact on bridge seismic fragility. Wibowo et al. (2012) conducted the large-scale shake table experiment with a single platoon of H-20 trucks as static live loads on the 2/5-scale three-span and horizontally curved bridge model. Most existing studies considered a single vehicle or a platoon of stationary vehicles, rather than moving vehicles as a part of realistic traffic flow.

As compared with short- and medium-span bridges, some promising progress has been made in terms of modeling moving vehicles on long-span bridges with or without seismic excitations (Chen and Wu 2010, 2011; Zhou and Chen 2015). Zhou and Chen (2014) proposed a fully coupled long-span bridge and traffic simulation framework based on the mode-superposition concept with detailed dynamic modeling of each vehicle and the bridge. With known limitations on incorporating nonlinearities, a mode-based approach may be appropriate for global seismic response prediction of long-span bridges due to limited local damage and nonlinearity of major bridge components. It is, however, not appropriate for the seismic performance prediction of short- and medium-span bridges, which often undergo considerable nonlinear

effects, local damages, and even total collapse of the bridge as a result of earthquakes, as discussed previously. Moreover, traditional nonlinear seismic analyses of short- and medium-span bridges have been successfully conducted using some commercial software, such as ANSYS, SAP2000, or open-source software like OpenSees. Although very versatile with nonlinear seismic analyses, existing commercial or open-source software, however, cannot directly incorporate complex dynamic interactions between multiple moving vehicles and bridges. Therefore, there is no appropriate methodology reported in literatures so far that can be used for nonlinear seismic analyses of typical short- and medium-span bridges while rationally considering the coupling effects between the bridge, moving vehicles, and earthquake at the same time.

### **1.3 Organization of This Report**

In the following sections, a new hybrid simulation approach is proposed to conduct the nonlinear seismic analysis of the bridge/traffic/earthquake system by integrating the stochastic traffic flow simulation, the mode-based fully-coupled simulation technique of the bridge-traffic system, and the nonlinear seismic analysis capabilities offered by OpenSees. A prototype bridge is studied as a demonstration under several earthquake scenarios, and the numerical analyses are conducted to provide some insights on the bridge's seismic performance and impacts of traffic.

## 2. MODE-BASED BRIDGE/TRAFFIC INTERACTION ANALYSIS

### 2.1 Stochastic Traffic Flow Simulation

The instantaneous temporal and spatial information of every single vehicle was obtained through the traffic flow simulation via the two-lane cellular automaton (CA) model (Chen and Wu 2011). The variables for each cellular were updated based on the vehicle information in adjacent locations and the probabilistic traffic rules regulating the accelerating, decelerating, lane changing, and braking, which can be referred to the study by Chen and Wu (2011). The CA-based traffic flow simulation was performed on a roadway-bridge-roadway system to simulate the stochastic traffic flow through the bridge in a more realistic way. Periodic boundary conditions were adopted in the traffic flow model, in which the total number of each type of vehicle in the roadway-bridge-roadway system remained constant. The vehicles in the stochastic traffic flow can be categorized into several representative types from a variety of vehicle configurations (Chen and Wu 2011).

### 2.2 Fully-coupled Bridg-traffic Interaction Model

The bridge and vehicles were modeled as two subsystems in the bridge-traffic dynamic interaction analysis system. The bridge subsystem was constructed based on the degrees of freedom (DOFs) in modal coordinates corresponding to the total number of the selected modes for the bridge. The vehicles were modeled as a combination of several rigid bodies, wheel axles, springs, and dampers. The vehicle subsystem was established with all the DOFs in physical coordinates of the vehicle dynamic models (Figure. 2.1). Detailed information for the vehicle dynamic model and the fully-coupled bridge-traffic interaction analysis can be found in the References (Zhou and Chen 2014, 2015). It was assumed that the tires of each vehicle and road surface have point contact without separation. The surface roughness of the approaching road and the bridge deck was modeled as a stationary Gaussian random process with zero mean value. The motion equations in a matrix form of bridge/traffic system can be expressed as follows:

$$\begin{aligned}
 & \left[ \begin{array}{ccccc} \Phi^T M_b \Phi & 0 & 0 & \cdots & 0 \\ 0 & M_{v_1} & 0 & \cdots & 0 \\ 0 & 0 & M_{v_2} & \cdots & 0 \\ \vdots & \vdots & \vdots & \ddots & \vdots \\ 0 & 0 & 0 & 0 & M_{v_n} \end{array} \right] \begin{Bmatrix} \ddot{\xi} \\ \ddot{q}_1 \\ \ddot{q}_2 \\ \vdots \\ \ddot{q}_n \end{Bmatrix} + \left[ \begin{array}{ccccc} \Phi^T C_b \Phi + \Phi^T \sum_{i=1}^n C_{bci} \Phi & \Phi^T C_{b,v_1} & \Phi^T C_{b,v_2} & \cdots & \Phi^T C_{b,v_n} \\ C_{v_1,b} \Phi & C_{v_1} & 0 & \cdots & 0 \\ C_{v_2,b} \Phi & 0 & C_{v_2} & \cdots & 0 \\ \vdots & \vdots & \vdots & \ddots & \vdots \\ C_{v_n,b} \Phi & 0 & 0 & \cdots & C_{v_n} \end{array} \right] \begin{Bmatrix} \dot{\xi} \\ \dot{q}_1 \\ \dot{q}_2 \\ \vdots \\ \dot{q}_n \end{Bmatrix} \\
 & + \left[ \begin{array}{ccccc} \Phi^T K_b \Phi + \Phi^T \sum_{i=1}^n K_{bci} \Phi & \Phi^T K_{b,v_1} & \Phi^T K_{b,v_2} & \cdots & \Phi^T K_{b,v_n} \\ K_{v_1,b} \Phi & K_{v_1} & 0 & \cdots & 0 \\ K_{v_2,b} \Phi & 0 & K_{v_2} & \cdots & 0 \\ \vdots & \vdots & \vdots & \ddots & \vdots \\ K_{v_n,b} \Phi & 0 & 0 & \cdots & K_{v_n} \end{array} \right] \begin{Bmatrix} \xi \\ q_1 \\ q_2 \\ \vdots \\ q_n \end{Bmatrix} = \left\{ \begin{array}{c} \Phi^T \sum_{i=1}^n F_{v_i}^G + \Phi^T F_b^r \\ F_{v_1}^r \\ F_{v_2}^r \\ \vdots \\ F_{v_n}^r \end{array} \right\}
 \end{aligned} \tag{1}$$

in which  $\mathbf{M}_b$ ,  $\mathbf{K}_b$  and  $\mathbf{C}_b$  are the generalized mass, stiffness, and damping matrices for the bridge structure, respectively;  $n$  is the number of vehicles traveling on the roadway-bridge-roadway system in the traffic flow;  $\mathbf{M}_{v_i}$ ,  $\mathbf{K}_{v_i}$  and  $\mathbf{C}_{v_i}$  are the mass, stiffness and damping matrices of the  $i^{\text{th}}$  vehicle in the traffic flow, respectively;  $K_{bci}$  and  $C_{bci}$  refer to the stiffness and damping contributions to the bridge

structure due to the coupling effects between the  $i^{\text{th}}$  vehicle in the traffic flow and the bridge system, respectively;  $\mathbf{K}_{b,v_i}$  and  $\mathbf{C}_{b,v_i}$  are the coupled stiffness and damping matrices for the bridge structure corresponding to the  $i^{\text{th}}$  vehicle in the traffic flow, respectively;  $\mathbf{K}_{v_i,b}$  and  $\mathbf{C}_{v_i,b}$  are the coupled stiffness and damping matrices for the  $i^{\text{th}}$  vehicle in the traffic flow corresponding to the bridge structure, which are equal to the transposed matrices of  $\mathbf{K}_{b,v_i}$  and  $\mathbf{C}_{b,v_i}$ , respectively;  $\xi$  is a vector of generalized coordinates of the bridge corresponding to each mode involved in the analysis;  $\Phi$  is the mode shape matrix of the bridge;  $q_i$  is a vector of the physical responses corresponding to each degree of freedom of the  $i^{\text{th}}$  vehicle in the traffic flow; one-dot and two-dot superscripts of the displacement vector denote the velocity and acceleration, respectively;  $\mathbf{F}_b$  and  $\mathbf{F}_{v_i}$  denote the external applied loads for the bridge in modal coordinates and the  $i^{\text{th}}$  vehicle in physical coordinates, respectively. The superscripts r and G denote the loads due to road roughness and self-weight, respectively.

The equations of motion were solved through the Newmark-Beta method in time domain, and the responses of the vehicles and the responses of the bridge corresponding to the generalized coordinates were obtained. Through the mode superposition of all the involved modes, the global physical response at any location of the bridge can be obtained from the full-coupled bridge-traffic interaction analysis, as shown in Eq. (2).

$$U^d = \sum_{j=1}^m \phi_j \xi_j = [\phi_1 \phi_2 \dots \phi_m] \{\xi_1 \xi_2 \dots \xi_m\}^T = \Phi \{\xi^d\} \quad (2)$$

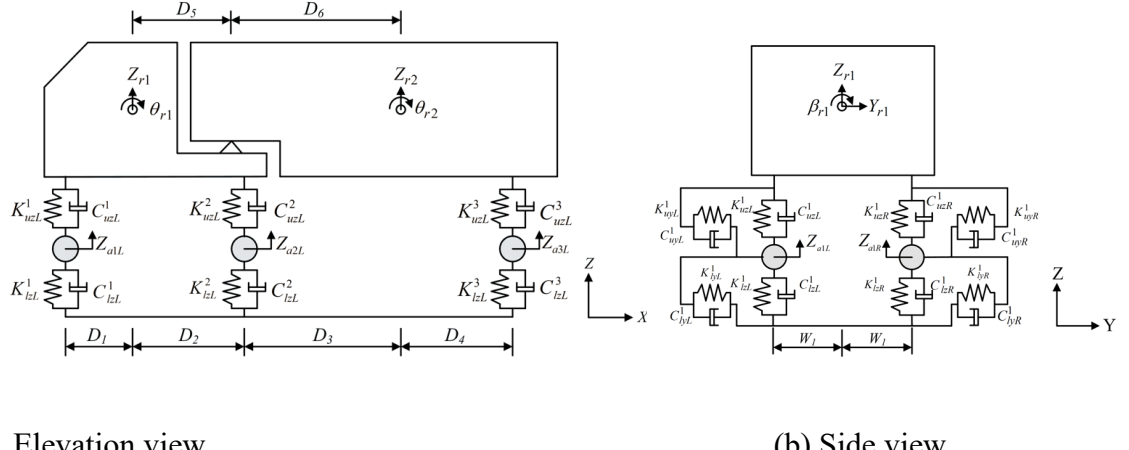


**Figure 2.1** The numerical dynamic model for the heavy truck with one trailer

### 3. HYBRID NONLINEAR SEISMIC ANALYSIS FRAMEWORK CONSIDERING TRAFFIC IMPACT WITH OPENSEES

#### 3.1 Equivalent Moving Traffic Loads (EMTL)

Considering that the elasticity and energy dissipation of the tires were modeled as springs and dampers in the lower locations of a vehicle, the dynamic wheel loads acting on the bridge structure are equal to the dynamic forces of the lower springs and dampers at the contact points. The equivalent wheel loads were obtained directly for each vehicle in the stochastic traffic flow from the time-history simulation results of the fully-coupled bridge-traffic interaction system as introduced above. The vertical and longitudinal equivalent moving traffic loads (EMTL) for the bridge girder nodes were further accumulated by distributing the equivalent wheel loads (EWL) for each vehicle using linear interpolation to the bridge girder nodes both longitudinally and transversely. The EMTL for each bridge girder node can be applied on the bridge structure in the finite element analysis model using OpenSees under multiple loading scenarios, in which both the material and geometric nonlinearities can be considered at the same time.

The vertical equivalent wheel load (EWL) for the  $i^{\text{th}}$  vehicle was determined as the summation of the vertical equivalent dynamic wheel loads and the gravity load:

$$F_{\text{ewl}}^{iz}(t) = F_{\text{edwl}}^{iz}(t) + G^i \quad (3a)$$

in which,  $G^i$  is the gravity load of the  $i^{\text{th}}$  vehicle;  $F_{\text{edwl}}^{iz}(t)$  is the vertical dynamic wheel load for the  $i^{\text{th}}$  vehicle in the traffic flow at time instant  $t$ , which is defined as (Chen and Cai 2007):

$$F_{\text{edwl}}^{iz}(t) = \sum_{j=1}^{na} (K_{lzL}^j \hat{Z}_{ajL}(t) + C_{lzL}^j \dot{\hat{Z}}_{ajL}(t) + K_{lzR}^j \hat{Z}_{ajR}(t) + C_{lzR}^j \dot{\hat{Z}}_{ajR}(t)) \quad (3b)$$

in which,  $\hat{Z}_{ajL(R)}(t)$  and  $\dot{\hat{Z}}_{ajL(R)}(t)$  are the relative vertical displacement and the corresponding first derivatives between the lower mass block on the vehicle at the left (right) side and the contacting point on the bridge, respectively;  $na$  is the total number of wheel axles for the  $i^{\text{th}}$  vehicle;  $K$  and  $C$  are the stiffness and damping coefficients of the springs and dampers in the vehicle model, respectively; the subscripts l, z, L(R) represent lower position, vertical (z) direction and left (right) side for the springs or dampers, respectively.

#### 3.2 EMTL-FE Hybrid Strategy

Figure 3.1 shows the flowchart of the proposed simulation strategy with three parts: (1) traffic loads, (2) OpenSees FEM model, and (3) scaled ground motions. For the traffic load part, the boundary conditions and driver behavior model of the CA-based traffic flow simulation were defined for the stochastic traffic flow simulation for a specific bridge and traffic scenario. With the simulated traffic flow results, the fully coupled bridge/traffic interaction analysis was conducted to provide time histories of the vertical equivalent wheel loads (EWL) for each vehicle of the traffic flow acting on the bridge under seismic loads. The EWL of each vehicle was linearly distributed in both longitudinal and transverse directions to the adjacent nodes of the bridge deck in the bridge finite element model in order to generate the cumulative time-dependent traffic loads acting on each node of the bridge deck, referred to as equivalent moving traffic loads (EMTL). The time-history excitations in vertical and longitudinal directions for each bridge deck node of the bridge finite element (FE) model can therefore be defined from the equivalent

moving traffic loads (EMTL). Extreme load excitations (e.g., seismic loads) can be applied to the bridge FE model (e.g., C) as the time-history inputs and the time-history nonlinear dynamic analysis is then conducted. Such a strategy is thus called “EMTL-FE hybrid strategy” because it integrates the fully coupled bridge-traffic dynamic analysis model through EMTL and the nonlinear finite element (FE) analysis with the nonlinear FE software.

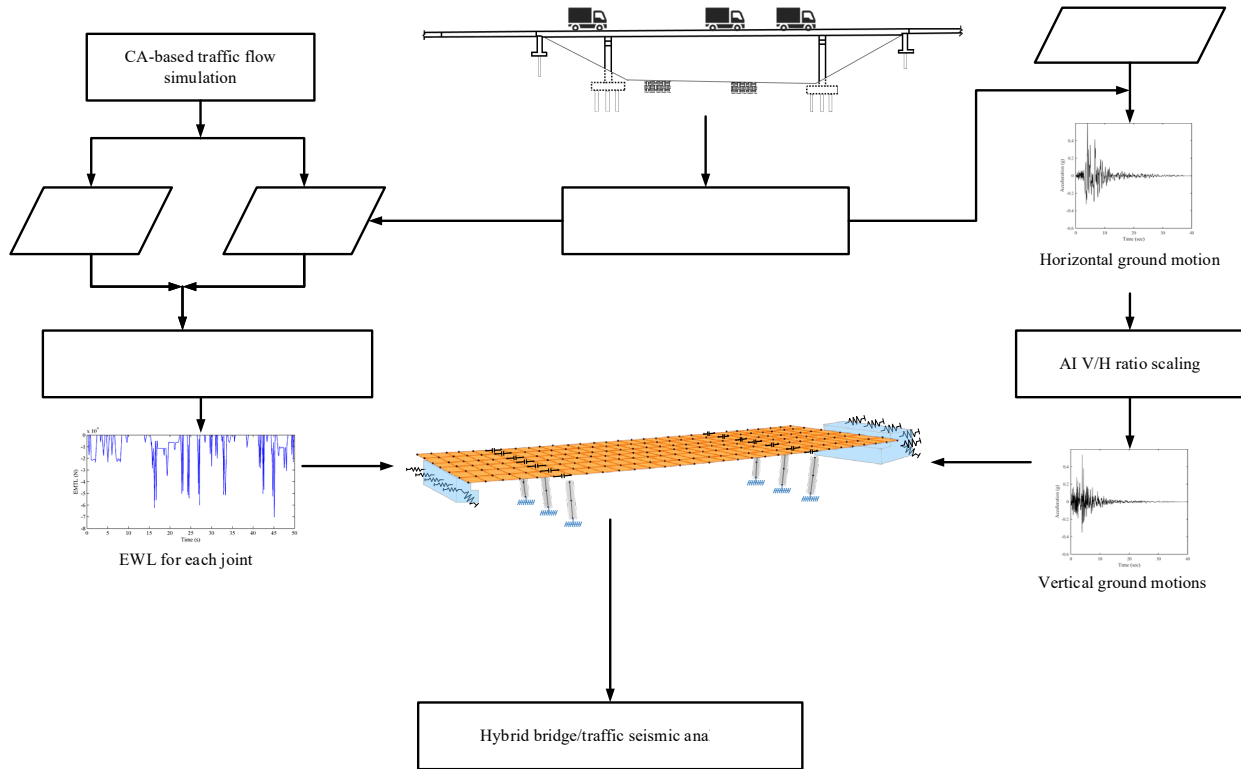
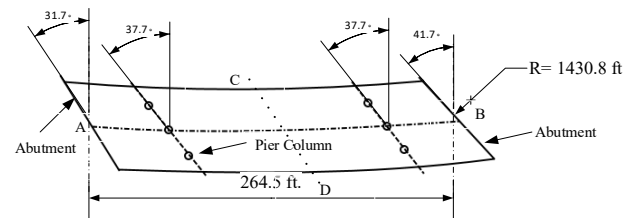


**Figure 3.1** Flowchart for EMTL-FE hybrid strategy

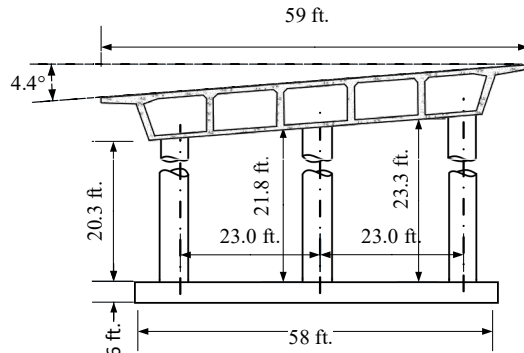
## 4. NUMERICAL INVESTIGATION OF PROTOTYPE BRIDGE

### 4.1 Prototype bridge and scenario earthquake records

Although the proposed methodology is applicable to all short- and medium-span bridges, a 3-span skewed and curved bridge, located in Tacoma Washington, is selected in this study as the prototype bridge to give greater insight into bridge seismic performance. The bridge location was considered as a moderate-to-high seismic region in the United States. The six-lane freeway bridge has a radius of curvature of 436.1 m and skew angles of 41.7 degrees and 31.7 degrees at both ends. As shown in Figure 4.1, the bridge deck is supported by concrete box girders over two sets of circular column bents, and connected with seat-type skewed abutments at both ends.



(a) Top view of girders



(b) Elevation view

**Figure 4.1** Geometries of prototype bridge and corresponding straight counterpart

The numerical model for the prototype bridge was constructed using the 3D finite element software “open system for earthquake engineering simulation (OpenSees)” (McKenna et al. 2006). The details of the 3-D OpenSees model for the prototype bridge, including some key connections, are shown in Figure 4.2.

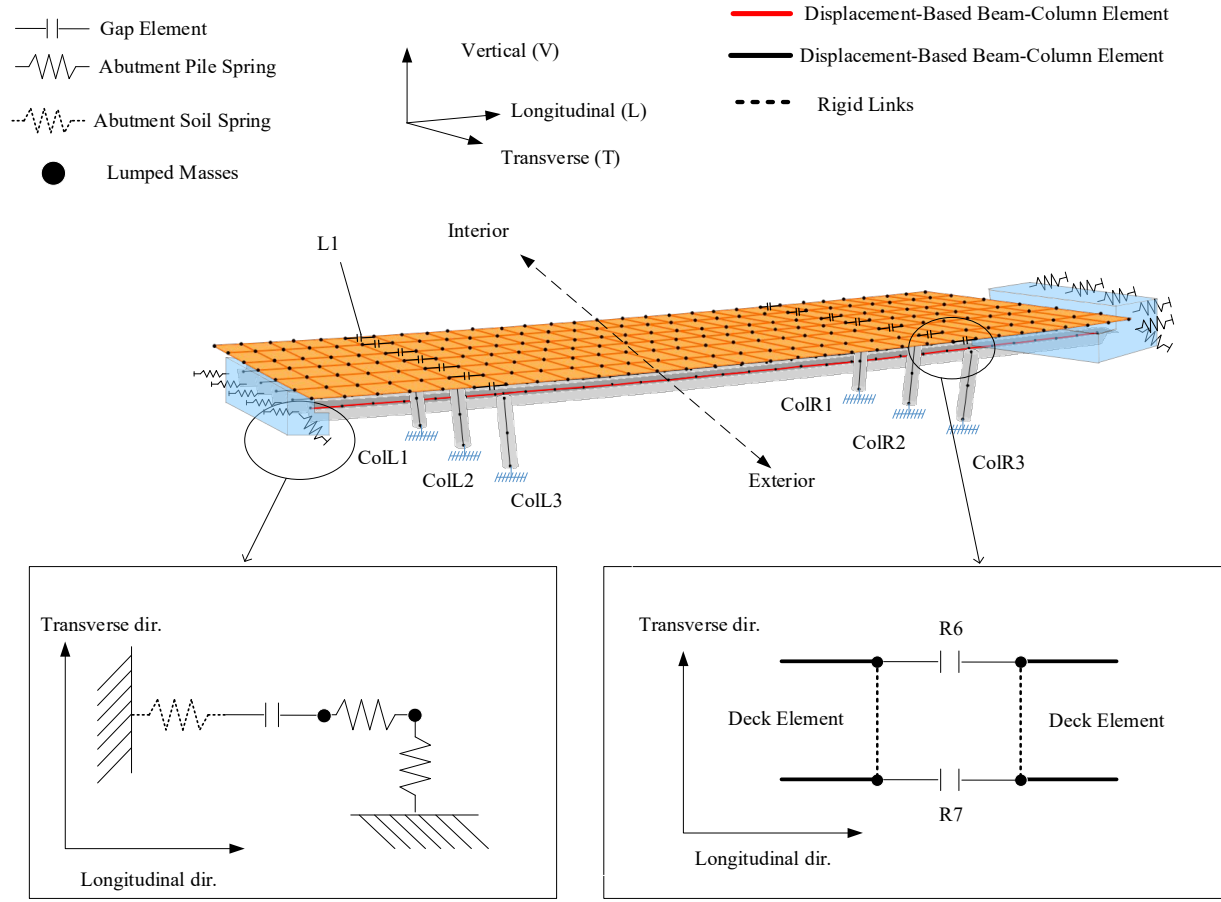


**Figure 4.2** 3-D OpenSees model of the prototype bridge

The circular reinforced concrete columns were modeled using fiber elements with modified uniaxial Kent-Scott-Park concrete material, which accounts for plastic behaviors after cracks occur during an earthquake (Stanton and McNiven 1979). In order to simulate the bridge/traffic interactions with detailed time-history inputs in the 3-D domain, the bridge deck elements were modeled in refined details with shell elements and elastic membrane plate sections, supported by five segments of elastic frame elements for box girders. Each segment has equivalent elastic properties of the prototype bridge girder since the bridge superstructure is usually deemed to remain elastic during seismic excitation. As shown in Figure 3, for each girder element, rigid link elements were used to connect the bridge deck and the girder element to ensure they share the same degrees of freedom (DOF) on the interface. The 0.5-inch expansion joints were modeled with gap elements on the deck above the column bent. For the abutments, the stiffness contributed from the piles in the active direction was modeled with the abutment pile springs, and the stiffness from the soil in the passive direction was modeled with additional soil springs connected to the pile springs, as shown in the bottom left of Figure 4.2 (Nielson 2005). Between the pile spring and soil spring, a 0.5-inch gap element was added to capture the available gap and for predicting the pounding forces between the girder-end and abutment. In the case study, the bridge model uses a Rayleigh damping matrix to define structural damping. A typical damping ratio of 5% is selected and assigned to the first two modes for defining the corresponding mass and stiffness proportional damping coefficients. The mass proportional damping and stiffness proportional damping are assigned to equivalent lumped-mass nodes and abutment link elements.

In order to evaluate the impact of traffic loads to bridges, this study considered vertical vehicle loads along with horizontal-vertical direction ground motions. According to some existing studies on earthquake characteristics (Newmark 1973; Kunnath et al. 2008), vertical ground motions were considered as those that come with lateral shear wave, and their magnitudes were generally dependent on the horizontal component of a seismic component, either in longitudinal or transverse direction. To keep the numerical demonstration within an appropriate scope, it was assumed that longitudinal ground motion was applied along with the vertical seismic component as the baseline case. A near-field record of the Northridge earthquake in 1994 was selected as the scenario earthquake excitation to justify the consideration of vertical ground motion as the scenario excitation set. Ground motion used in this study was scaled following the method adopted by Wilson et al. (2015) based on its peak ground acceleration (PGA), in which the longitudinal component was scaled to match the seismic design spectrum, while the vertical component was scaled accordingly by keeping the same Arias Intensity ratio (Table 4.1). The scaled time histories of longitudinal and vertical seismic accelerations are shown in Figure 4.3.

**Table 4.1** Scenario ground motion selection

Event	Mw	Type	Station	R <sub>rup</sub> <sup>*3</sup> (km)	L <sup>*4</sup> (sPGA <sup>*2</sup> )	V <sup>*5</sup> (sPGA)
<b>Northridge</b>	6.7	NF <sup>*1</sup>	Sylmar - Olive View Med FF	5.30	0.57	0.22

Note: \*1: NF=Near-fault earthquakes; \*2: sPGA=Scaled peak ground acceleration; \*3: R<sub>rup</sub>= Closest distance to the fault rupture plane; \*4: L =longitudinal direction; \*5: V= vertical direction.

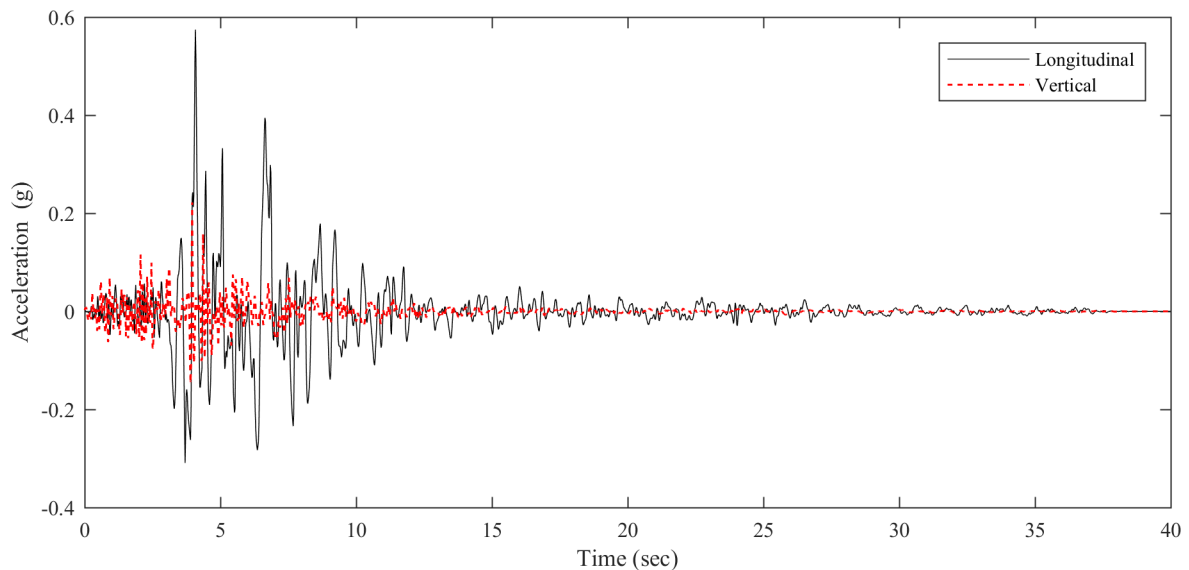


**Figure 4.3** Scenario seismic excitation

## 4.2 Traffic Loads from Bridge-traffic Interaction Effects

Traffic flow was assumed to be “busy traffic” with a density of 32 vehicles/km/lane for three lanes, which are the fast lane, middle lane, and slow lane. The relative location between the traffic lanes and the girders is shown in Figure 4.4.

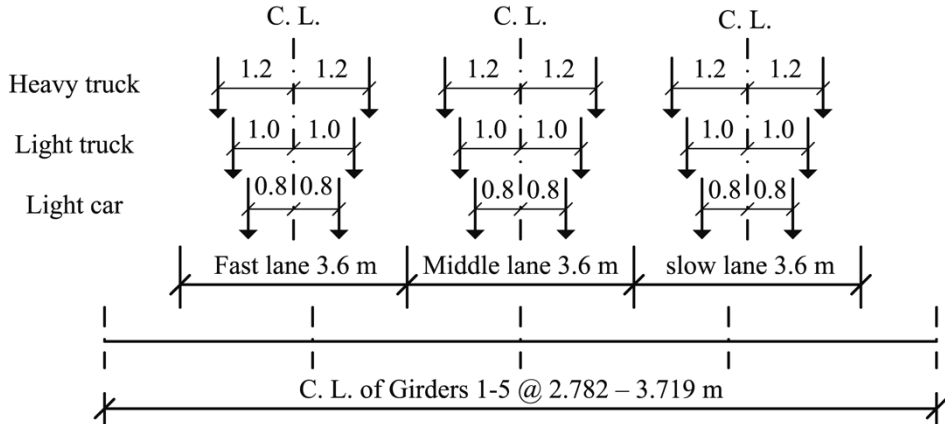


**Figure 4.4** Side view of the vehicle wheels on the traffic lanes for the prototype bridge

The percentages of the three types of vehicles in the traffic flow were assumed to be 25%, 25%, and 50% for heavy trucks, light trucks, and light cars, respectively, representing a typical vehicle composition in the traffic flow. The total length of the roadway-bridge-roadway path was 247.5 m, including two roadway segments with a length of 82.5 m each and the bridge in a length of 82.5 m. The simulated stochastic traffic flow at the busy traffic condition consisted of 24 vehicles in the roadway-bridge-roadway system, including six heavy trucks, six light trucks, and 12 light cars. The total DOFs of the bridge-traffic system was 390, in which the first 60 DOFs were in the modal coordinates of the bridge corresponding to the first 60 modes, and the later 330 DOFs were in the physical coordinates for all the vehicles. The busy traffic flow was simulated stochastically with a duration of 40 seconds based on the spatial information of bridge deck and traffic flow density in Figure 4.5, which shows the longitudinal locations of the vehicles with respect to time on the fast lane of the bridge in the traffic flow.

Representative EMTLs at the center of the main span and west side span on the bridge deck are given in Figures 4.6(a) and (b), respectively. The EMTL values varied significantly with respect to time due to the movement of vehicles in the traffic flow, and those values in the main span and side span were similar in terms of magnitude.

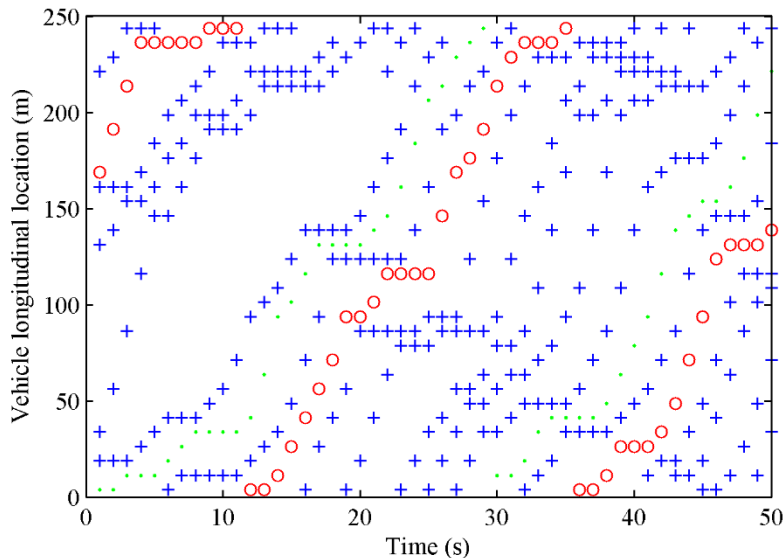


**Figure 4.5** Longitudinal locations of the vehicles on the fast lane in the busy traffic flow  
(+ = light cars, O = light trucks, ●=heavy trucks)

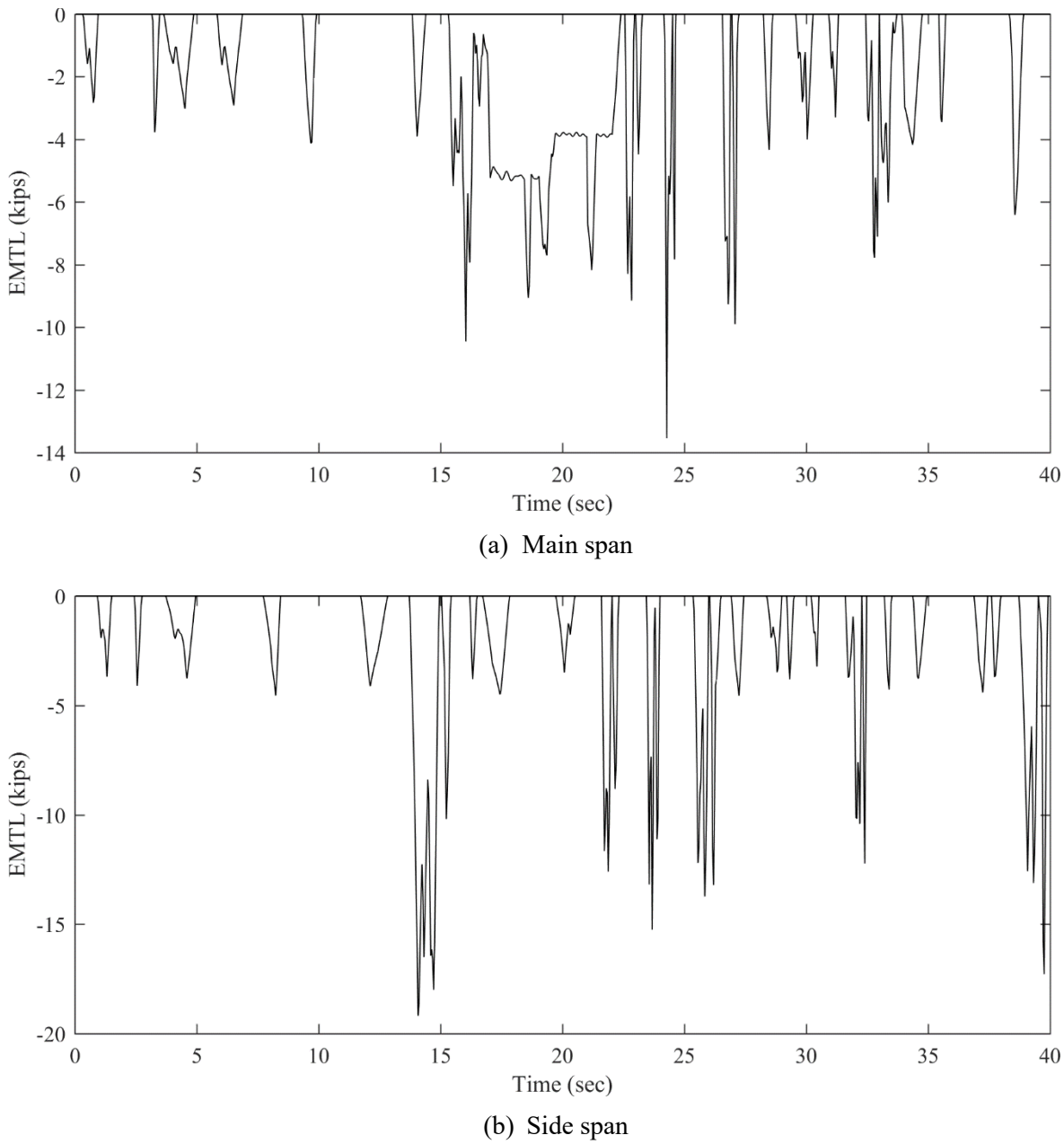


**Figure 4.6** EMTL at the center location of the span on the skewed bridge deck

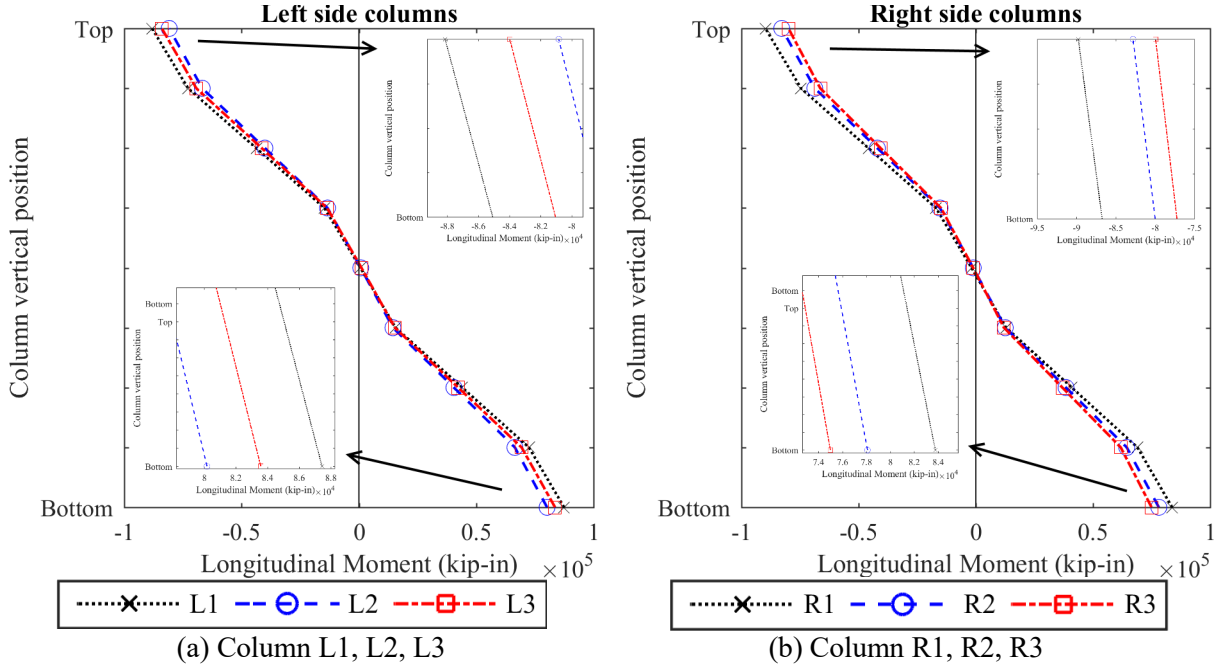
### 4.3 Nonlinear Seismic Analysis Results

The EMTL time histories obtained from the mode-based interaction analysis were applied to the corresponding bridge deck joints of the OpenSees model as inputs (Figure 4.2). For intermediate nodes of the bridge deck in both transverse and longitudinal directions, linear interpolation was applied to the EMTL to generate the time history inputs for adjacent nodes. Note that in this study, EMTL derived based on normal bridge-vehicle interaction was applied for the bridge nonlinear seismic analysis, with the following two approximations:

- 1) The EMTL on the bridge is obtained from bridge-traffic interaction analysis (Zhou and Chen 2015), which assumes that the vehicle wheels have point contact with the bridge deck without separation. It is a necessary mathematical assumption in order to directly couple the bridge and each individual vehicle in the traffic flow. It is beyond the scope of state-of-art research to realistically model the separation, reconnection, and the coupling between the wheel and bridge deck in a single dynamic analysis due to the nature of dynamic equations.
- 2) The driving behavior of the traffic flow when a seismic event occurs was assumed to be same as normal condition. Based on several studies of driver behavior on bridges during several seismic events, it was reported that drivers usually realize the occurrence of seismic events and then apply braking only when the seismic intensity is very high (Maruyama and Yamazaki 2006). For short- and medium-span bridges, the passing time of vehicles through the bridge is usually short, which may not allow the drivers to take action while they still remain on the bridge after the initial reaction time. Furthermore, there is lack of a general and well-accepted driving behavior model to characterize the driver response during earthquakes with different intensities. To propose a general approach for all seismic scenarios, the driving behavior change during the earthquake is ignored in this study.

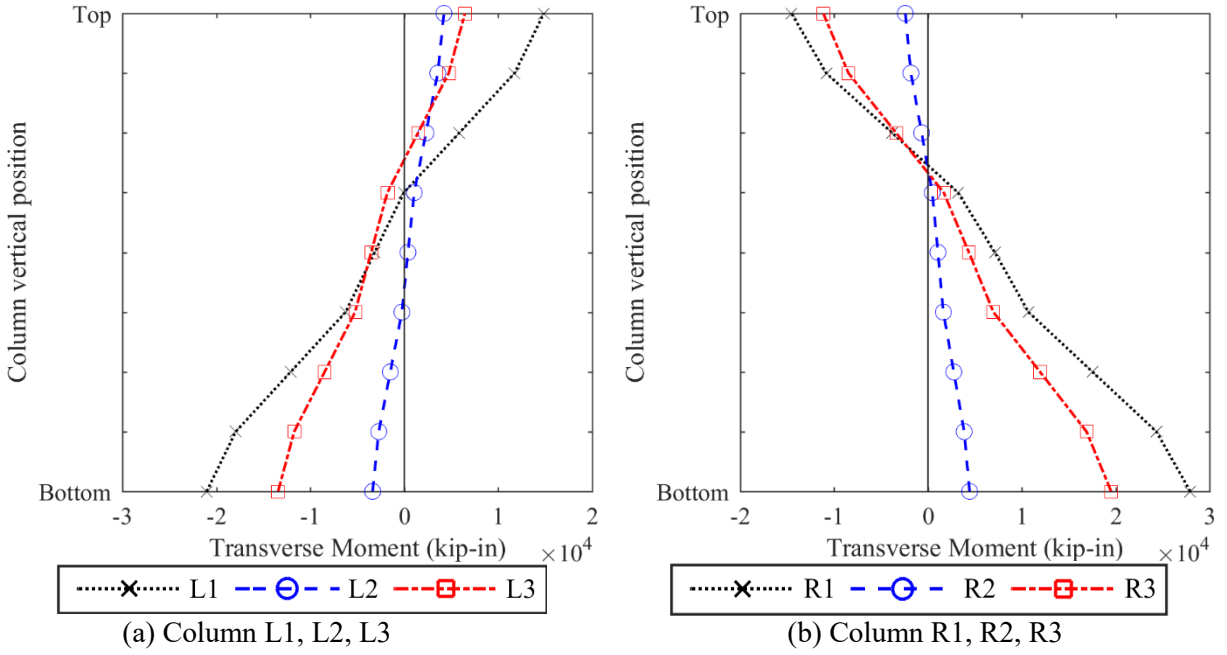
Nonlinear time-history seismic analysis was then conducted on the OpenSees FEM model where the seismic inputs were applied at the base of the columns and the traffic inputs applied on the bridge deck. The nonlinear time-history analysis used direct integration of the Hilber-Hughes-Taylor method with alpha, beta, and gamma values of 0.0, 0.25, and 0.5, respectively. The analysis results of different bridge components are discussed in the following section.

In general, bridge columns are one of the critical components for bridge seismic analysis due to relatively higher vulnerability to damage than the superstructure. According to previous studies, the most common structural failure modes for columns can be categorized as displacement ductility (Sivaramakrishnan 2010; Nikoukalam and Sideris 2016) and drift ratio (Fahmy et al. 2010; Ghobarah 2001). Existing studies showed that different columns usually have different seismic performance for a skewed and curved bridge (Wilson et al. 2015; Chen and Chen 2016). The seismic response of all the columns are discussed in the following sections and the most critical column may be identified as a representative one for further discussions. Figures 4.7 and 4.8 give the maximum longitudinal and transverse moments for six columns respectively, and the definitions of the column numbers can be found in Figure 4.2. Longitudinal moments of the columns are fairly close among those three columns on the left side (L1-3) and also the three on the right side (R1-3), as shown in Figure 4.7 (a-b). The zoomed-out view of the moments in Figure 4.7 (b) shows slight a difference for different columns on each side, and column L1 (ColL1) is found to have the maximum longitudinal moment among all the columns and the moments for all the columns on the left.



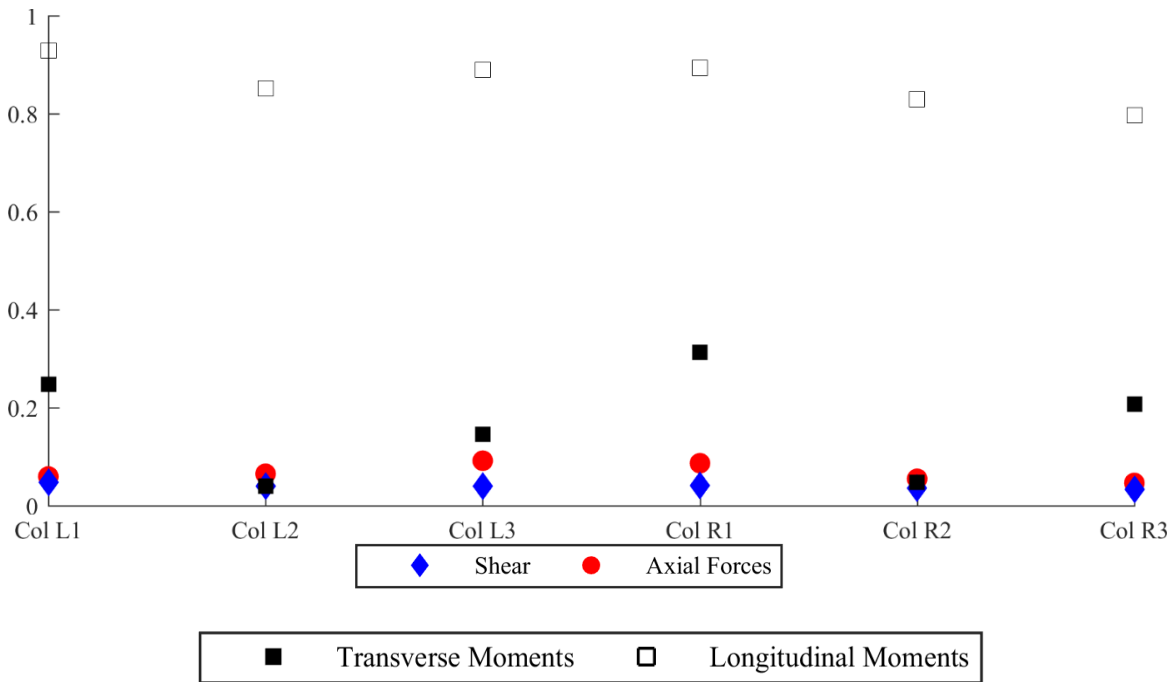
**Figure 4.7** Longitudinal moments of individual columns

Figure 4.8 shows that the left-side columns (L1-L3) have slightly higher transverse moments than those of the right-side columns (R1-R3). For the columns on the same side, it is obvious that the transverse moments of different columns vary considerably (Figure 4.8). For example, for the left-side columns, column L1 can achieve over four times the transverse moments at both ends than those of column L2. Similar trends can also be observed for the right-side columns (i.e., R1-R3). The transverse moments of columns vary considerably between the interior column (L3) and the exterior one (e.g., L1) on the same side. All the differences of the longitudinal and transverse moments on different columns are caused by the skew, curvature, and superelevation nature of the bridge; and the findings suggest that specific design of individual columns for skewed and curved bridges may be warranted to achieve both robust and economical designs.



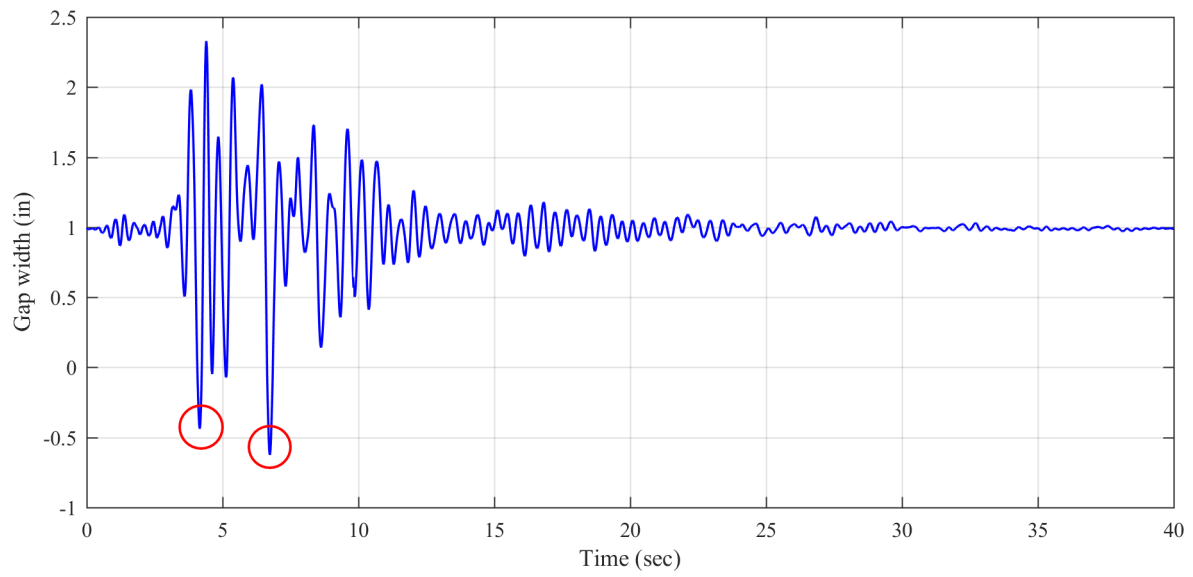
**Figure 4.8** Transverse moments of individual columns

Figure 4.9 summarizes the demand and capacity (D/C) ratio for shear, axial forces, transverse moments, and longitudinal moments for all six columns. It is found the D/C ratios of both axial force and shear are very small for all the columns, showing very large safety margins. It is found that D/C ratio for the transverse moment is quite small, i.e., around 0.2 to 0.3, which is understandable considering the horizontal seismic excitation was only applied in the longitudinal direction. In contrast, the D/C ratios for longitudinal moments of different columns are much higher (around 0.9). Among different columns, it is found that column L1 (Col L1) and column R1 (Col R1) have relatively larger transverse and longitudinal moments. By looking into the seismic response results of all the columns shown in Figures 8-10, it is concluded that column L1 (Coll1) has the largest overall seismic response for most of the cases, and is therefore selected as the representative column in the following discussion.



**Figure 4.9** Column demand/capacity ratio for individual columns

The longitudinal pounding forces between the concrete components during seismic events, such as shear keys, girder ends, and abutments, could induce spalling or crushing damage of concrete, as well as damage to the expansion joints. Such an issue has been studied in several previous researches (DesRoches and Muthukumar 2002; Muthukumar 2003; Chouw and Hao 2008; Shrestha and Bi 2013) and is also investigated in the following. In Figure 4.10, the variations of the gap width between the abutment and the girder on the right side over time are displayed with the gap width below 0 marked with red circles. As shown in Figure 4.11, at the corresponding time instants with negative values of the gap width, large pounding forces over 1,000 kips were observed. Without conducting detailed concrete damage assessment due to the scope limit, it is expected that considerable damage to the expansion joints and concrete on the girders and abutment would occur under such large pounding forces.



**Figure 4.10** Girder-abutment gap width between girder and abutment

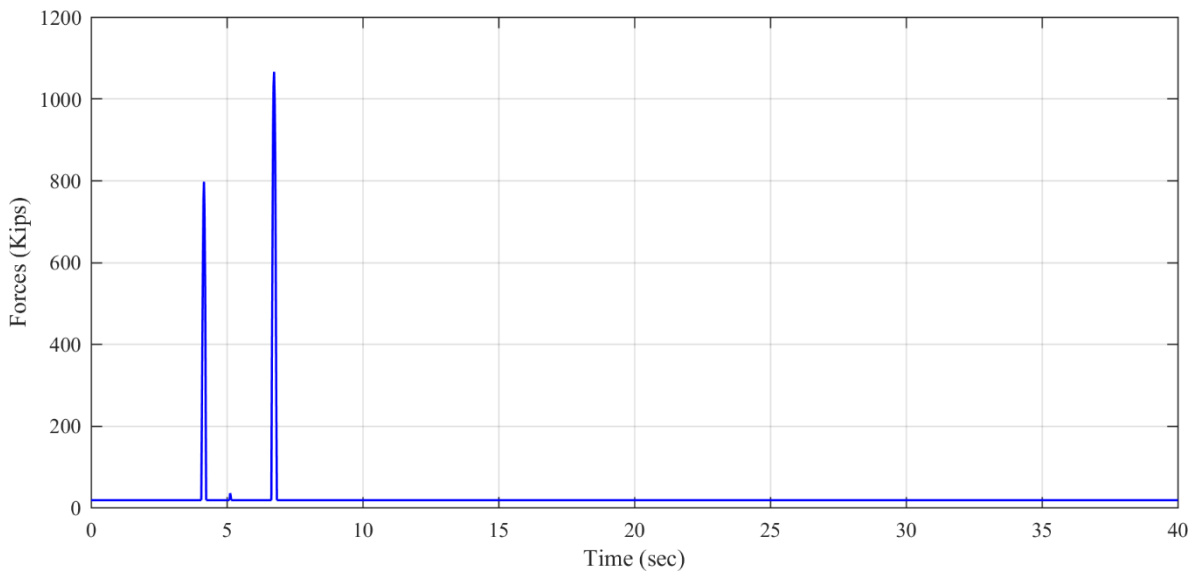


**Figure 4.11** Longitudinal pounding forces between girder and abutment

## 4.4 Impact of Different Excitation Scenarios of Ground Motions

In general, ground motions are characterized and quantified in three primary directions, including vertical component and biaxial combination of two orthogonal horizontal components following the 30% rule (Rosenblueth and Contreras 1977), 40% rule (Newmark 1975), or CQC3 (Menun and Kiureghian 1998), which have been adopted in many seismic design codes (ICBO 1997 and ASCE 1986).

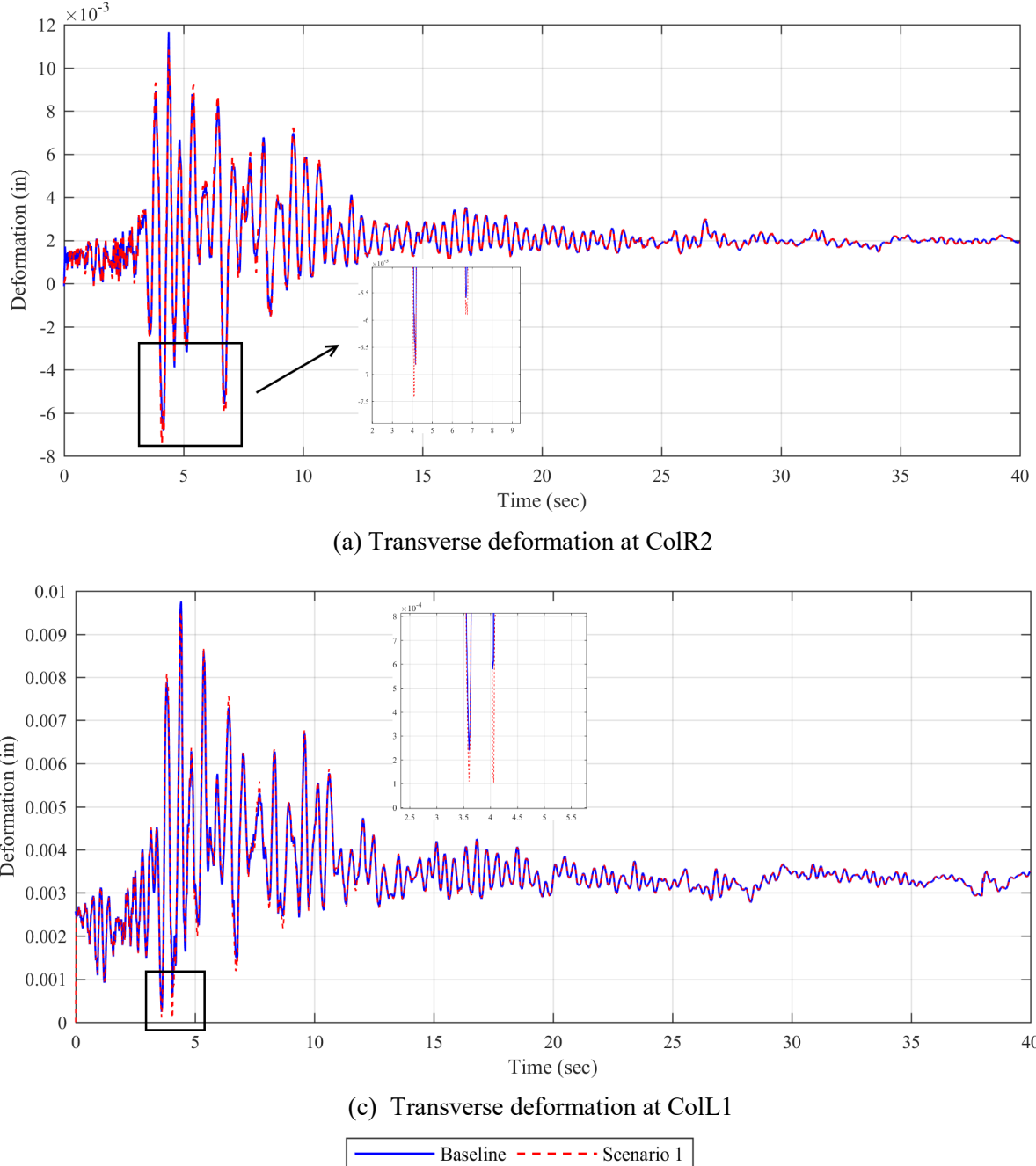
In this study, the baseline scenario (baseline) includes a 100% longitudinal component and a 100% vertical component. To study the impact from the transverse ground component, Scenario 1 is also studied by combining the longitudinal and transverse ground components following the 40% rule, along with the vertical component. Details about the ground motion input directions (record file names SYL090 and SYL-UP from PEER strong ground motion database) for each directional combination are listed in Table 4.2.

**Table 4.2** Input direction and intensities of different scenarios

Scenarios	Longitudinal	Transverse	Vertical
Baseline	100% SYL090	N/A	100% SYL-UP
Scenario 1	100% SYL090	40% SYL090	100% SYL-UP

Note: SYL090: Excitation in longitudinal direction; SYL-UP: Excitation in vertical direction

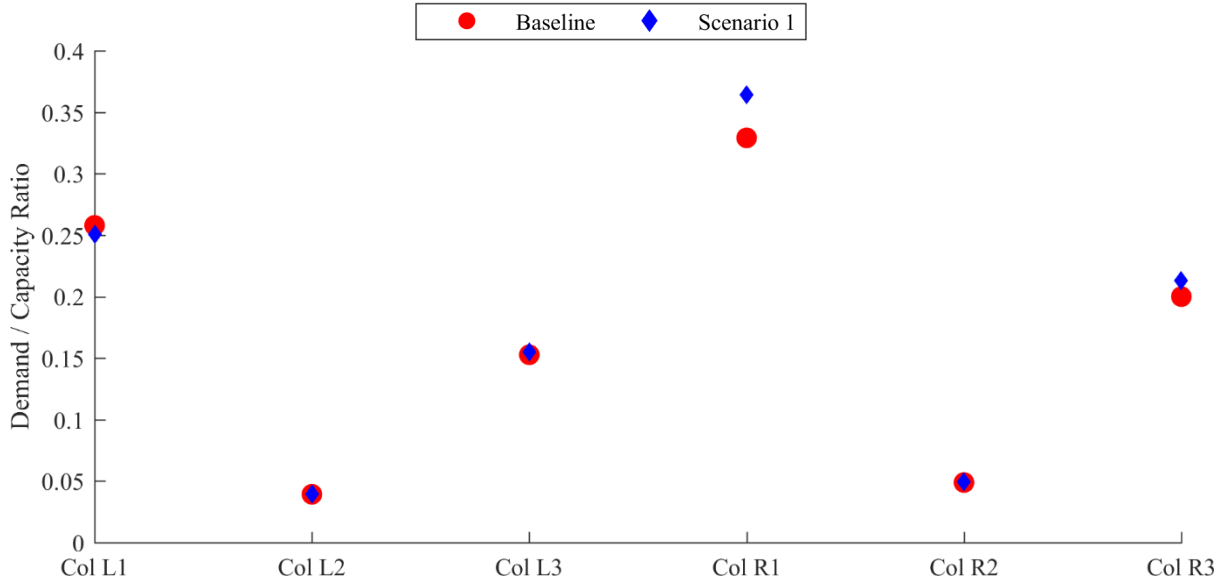
Comparative results of both scenarios are shown in Figures 4.12 (a) and (b). Although the absolute difference between two case results seems small since the PGA of the transverse component of earthquake is 0.22g (40% of longitudinal earthquake), the deformation increment percentage can range from 8.82% (ColL1) to 81.75% (ColR2) at the diagonal locations being picked from Figure 4.2. This shows a possibility that specific structural designs in the transverse direction, such as for wingwall or shear keys, may need to be considered specifically to avoid possible excessive deformation.



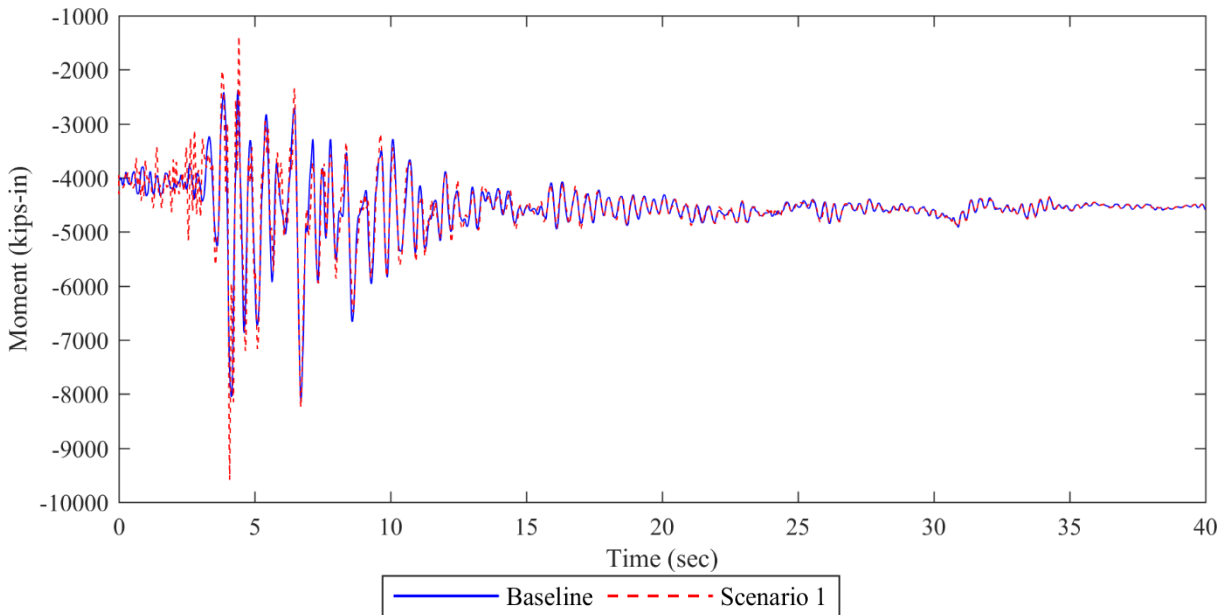
**Figure 4.12** Transverse deformation of columns

Figure 4.13 (a) shows the demand-capacity ratio of different columns under two scenarios, and it is found that the addition of transverse earthquakes results in different levels of increase of transverse moments among different columns, and the largest increment of column transverse moment is about an 18% increment on ColR1 [Figure 4.13 (a)]. The results suggest that even a small PGA of transverse earthquake (about 0.27 g) can still make a considerable difference on the column moments. Figure 4.13 (b) shows the time history of transverse moments of ColR1. Since the input ground motion characteristic is near-fault pulse-like ground motion, one can see that most of the difference of the two scenarios has been observed

during the first 15 seconds. Once the earthquake started to decapitate over time, the results of two scenarios become very similar.



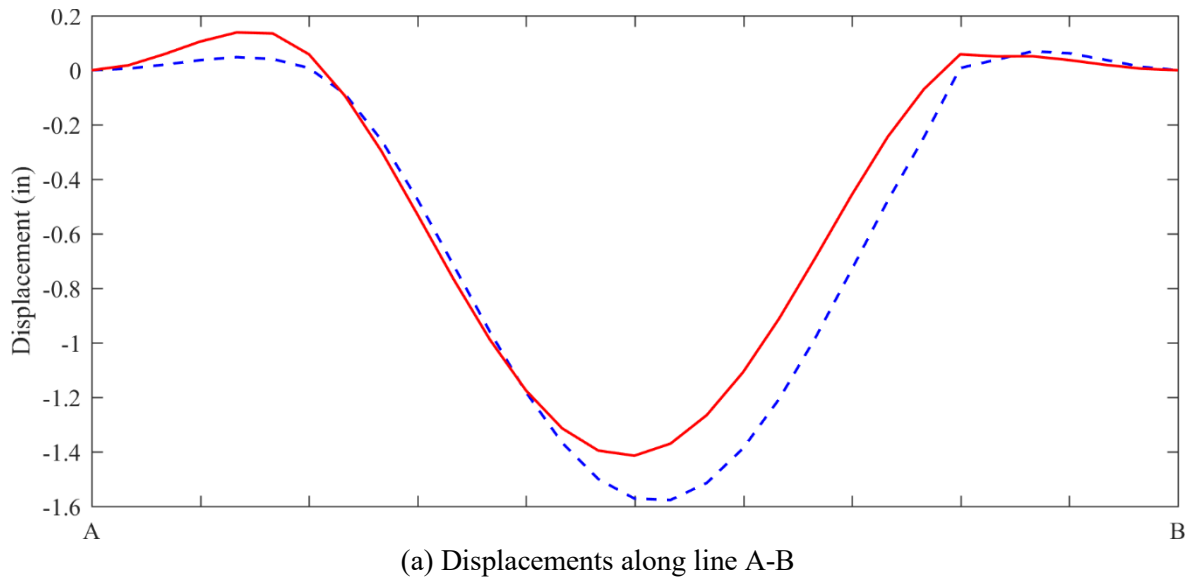
(a) Transverse moment D/C ratio comparison among different columns



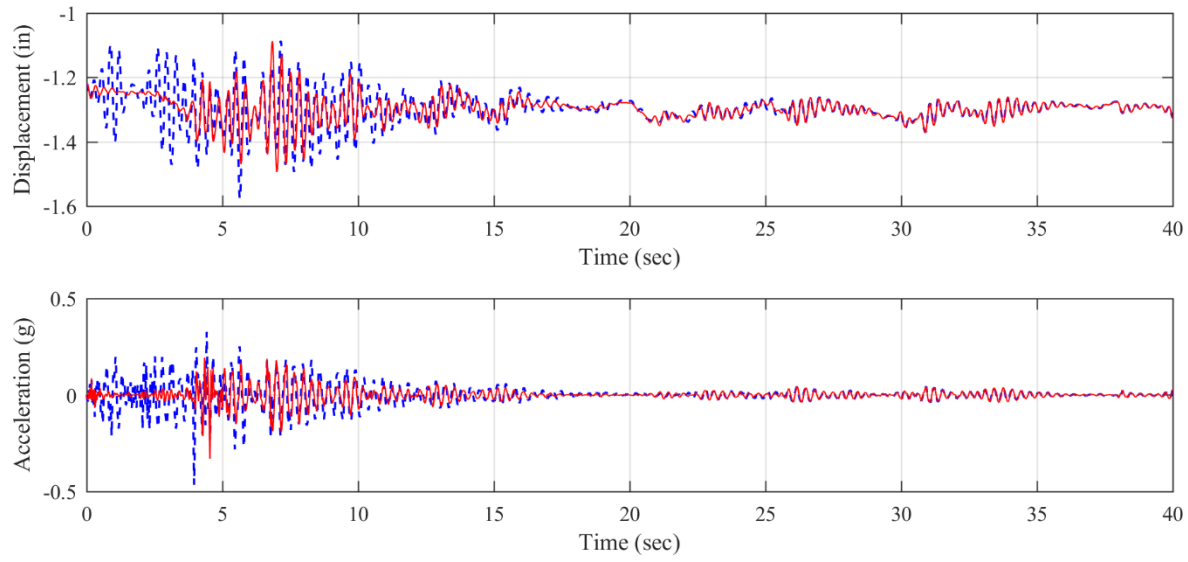
(b) Transverse moment time history of ColR1

**Figure4.13** Transverse moment comparison of columns

For the vertical displacement distribution along line A-B on the bridge deck, it is found that the addition of the transverse earthquake actually causes smaller vertical deck displacement and acceleration than the baseline case, as shown in Figures 4.14 (a) and (b).



(a) Displacements along line A-B



(b) Displacement and acceleration at midspan

—	Baseline	- - -	Scenario 1
---	----------	-------	------------

**Figure 4.14** Deck vertical response comparison

## 4.5 Impact of Traffic on Seismic Response

In normal conditions, traffic loads can cause considerable impacts on vertical displacements of the bridge deck and responses on bridge columns. As discussed earlier, the impact of realistic moving traffic on the bridge seismic response, however, was not clear. In this section, some comparative studies are conducted to look into such impacts. Since traffic loads and dynamic interactions primarily act in the vertical directions, the column response and vertical deck displacement response will be specifically studied in addition to other column responses.

### Column Response

As shown in Figures 4.15 (a) and (b), for the scenario earthquake with a high PGA, the traffic load only slightly affects the peak and residual column drift ratios, regardless of the possible longitudinal moment induced by superstructure curvature with vertical vehicle loadings. This is understandable since the traffic dynamic interactions mainly occur in the vertical directions of the bridge. However, since the longitudinal moment and drift ratio are critical seismic responses, often with very narrow safety margins, any small increase of the seismic response by the inclusion of traffic load should not be overlooked.

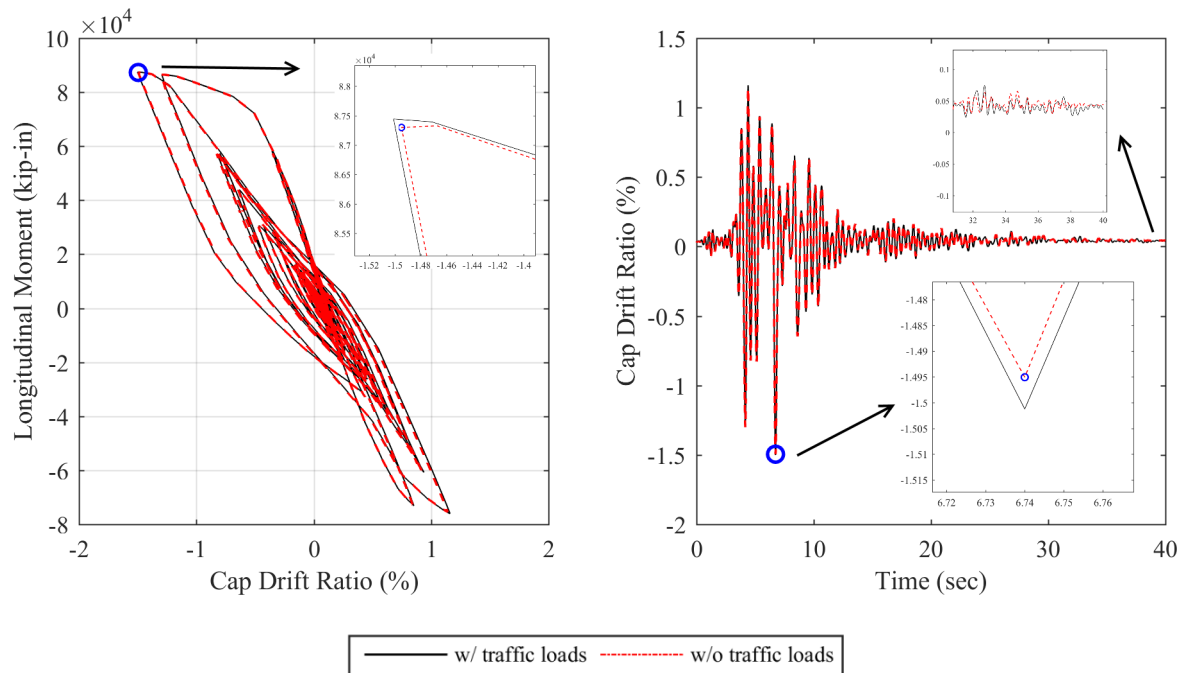


**Figure 4.15** Traffic effect to column Coll1 (a) Hysteresis loop (b) Drift ratio time history

The column axial forces of Coll1 were compared between those when the traffic load was considered and when it was not. As shown in Figure 4.16 (a), with the inclusion of the vertical traffic loading, column Coll1 has an increase of 3.48% on the peak axial force. As shown in Figure 4.16 (b), in addition to the seismic peak response, the traffic loads can contribute considerably to the residue response and when the seismic load is gradually dissipated. For some bridges with limited safety margins and being vulnerable to progressive damage following initial local damage or during aftershocks, the traffic impact can become significant.

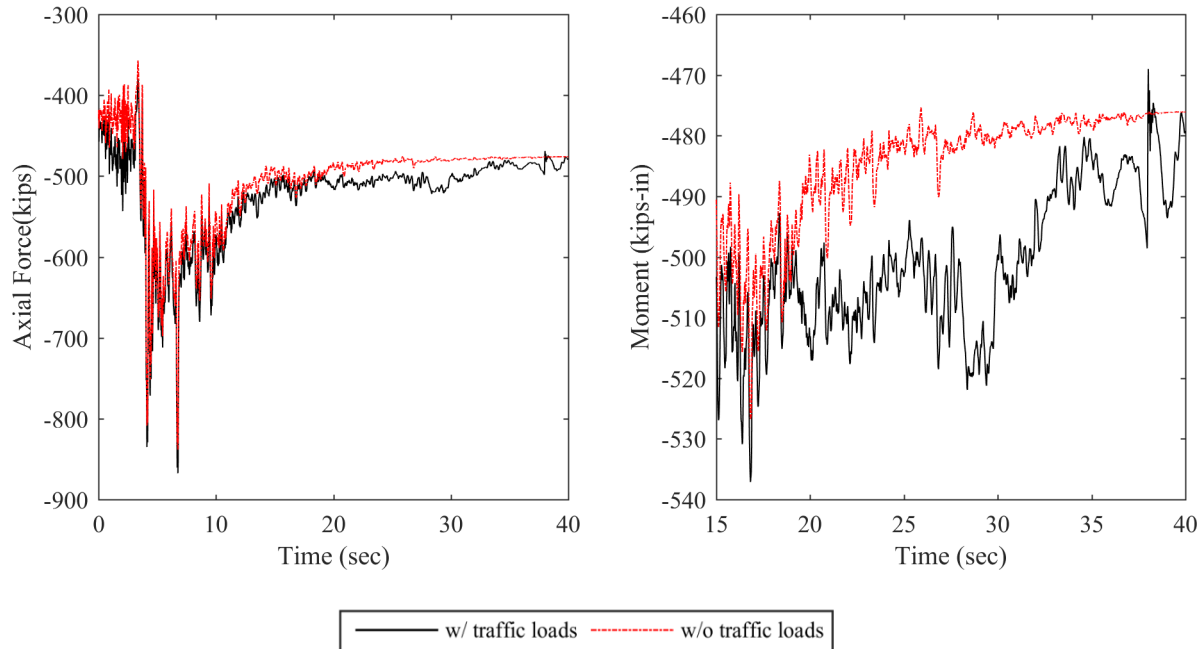


**Figure 4.16** Traffic effect to column ColL1 (a) axial forces (b) Zoomed out view

### Bridge Deck Response

As shown in Figure 18(a), comparisons of the vertical peak displacements were made along the longitudinal and transverse lines A-B and C-D (marked on Figure 4.1), respectively, in the middle span of the bridge. The peak vertical displacement reaches 1.57 inches with the inclusion of traffic loads, which is 5.63% higher than the one when the traffic load is excluded. In terms of the mean displacement, the traffic load causes increments of 5.69% and 5.30% along line A-B and line C-D, respectively, due to the off-center deck curvature and expansion joints.

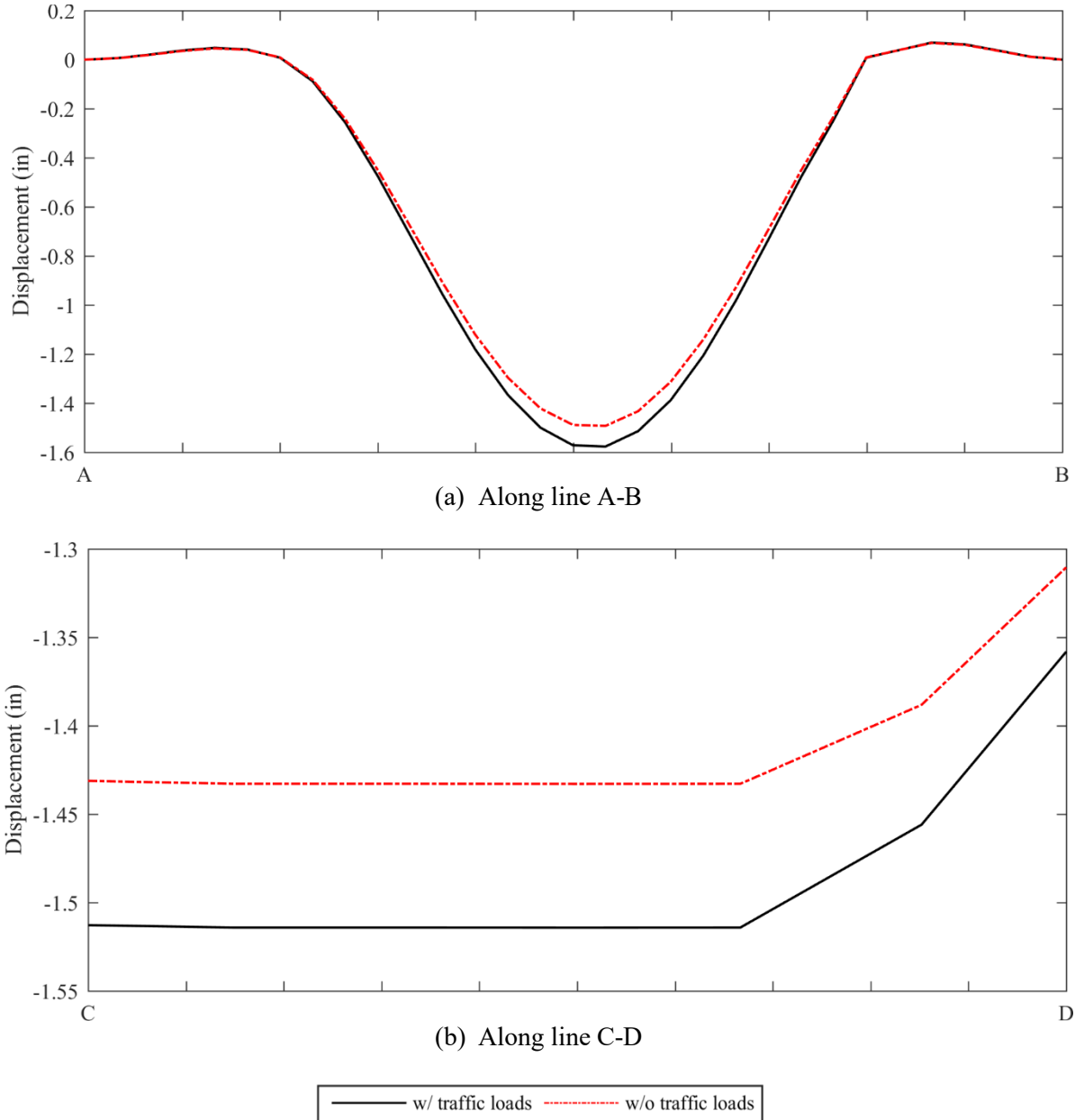


**Figure 4.17** Deck peak vertical displacements

Under the scenario seismic load, the impact of traffic loads on the bridge vertical displacement was further studied. Figure 4.18 (a-b) shows the time history results of the vertical displacement and the acceleration at the middle point of the bridge, respectively. On each subplot, the results with and without the inclusion of traffic loads were compared. Figure 4.18 (a) shows that the inclusion of the traffic load in the seismic analysis of the prototype bridge can cause considerable increase of the vertical displacement from 1.51 to 1.58 inches (an increment of 5.63%) even during the time instants when the seismic-induced response reaches the maximum. As shown in Figure 4.18 (b), the bridge vertical acceleration responses exhibit different patterns from those of the displacement. The maximum vertical acceleration with traffic loads is about 3% less than that without traffic loads due to the dynamic coupling effects. After roughly 15 seconds, the acceleration response caused by the earthquake becomes very mild, and the contribution from the traffic excitations becomes dominant and exhibits small fluctuations on the time-history

response. Comparatively, the existence of traffic loads can cause 11% larger bridge acceleration than that without traffic, which is mainly caused by the dynamic interactions between the bridge and moving vehicles.

The results suggest that the bridge seismic response considering the existence of traffic is more complex than simply superposing the responses of respective loads. The vertical displacement result is generally increased by the presence of the traffic almost all the time, while the acceleration result is only increased by the presence of the traffic when the seismic excitation becomes less significant. The pattern of the bridge acceleration response may suggest that the impact of traffic during the later stage of the seismic excitation can be critical, especially when some local damages may have already occurred. Although the absolute percentage value of the increment is not large, it may cause considerable difference in terms of the prediction accuracy of the potential damage on some bridge components when some members are already on the verge of damage or failure. For extreme loads induced by seismic excitation, such an increase can make a difference in terms of the seismic performance depending on the remaining safety margins for different bridge components under seismic events.

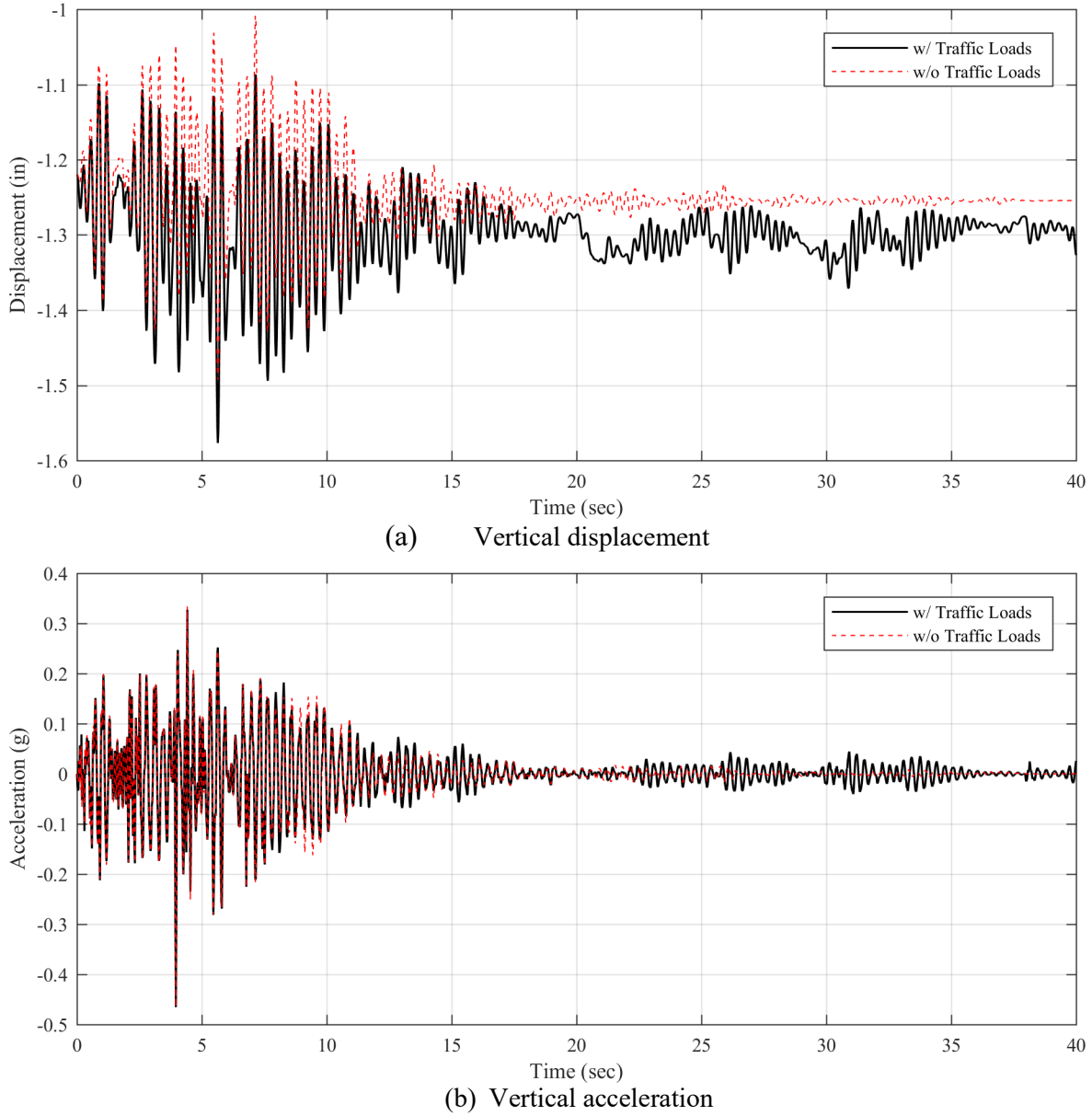


**Figure 4.18** Traffic load impact on vertical displacement and acceleration response at midspan

## 5. CONCLUSION

A hybrid nonlinear seismic analysis approach was proposed for short- and medium-span bridges considering dynamic interactions with moving traffic by taking advantage of both mode-based bridge/traffic interaction analysis and nonlinear FEM seismic analysis with OpenSees. A skewed and curved bridge under a scenario seismic input was studied for demonstration purposes. The baseline scenario, including vertical and longitudinal seismic inputs, were considered along with moving traffic in this study to demonstrate the proposed approach and provide insights of the bridge seismic response. Due to the lack of experimental data, a direct validation of the proposed approach is not yet possible.

For comparison purposes, the other scenario with the addition of transverse excitation was also studied. Numerical studies of the prototype bridge suggest that the proposed hybrid methodology can capture the complex dynamic interactions between the bridge and multiple vehicles, as well as nonlinear bridge seismic performance at the same time. Some observations from the numerical simulation results of the prototype skewed and curved bridge under the particular scenario earthquake are made as follows:

- The skewed and curved bridge has very different seismic responses on different columns under both seismic and traffic loads, such as transverse moments due to the curved and skewed nature. The demand and capacity ratio of the longitudinal moments is much higher than other seismic response, indicating limited safety reserve.
- There are large pounding forces between the girder and abutment, which may cause considerable damage to the concrete and expansion joints.
- The comparison between the results of the prototype bridge substructures with and without considering traffic disclosed some interesting observations. The impact from traffic on bridge seismic response is more complex than simple superposition of the responses under individual loads. For this particular scenario earthquake excitation, the consideration of traffic causes little increase on the peak values of some seismic performance of the columns, such as end moments and drift ratios. The impacts on the axial forces of the columns become more significant on both extreme values and the residue response. These findings confirm that traffic impacts mainly apply to the seismic response in vertical directions.
- Compared with the impact on the seismic response of substructures, traffic impacts on the performance of superstructures, such as vertical displacement and acceleration, are more significant. Overall, traffic load has considerable impact on the overall seismic peak response, even under the peak seismic response. It has a rather significant contribution to the residue response and also when the seismic load is gradually dissipated.
- Traffic may cause a considerable difference in terms of prediction accuracy of the potential damage on some bridge components when some members are already on the verge of damage or failure. The traffic impact can become critical for some bridges with limited safety margins and being vulnerable to progressive damage following initial local damage or during aftershocks.

The proposed methodology was demonstrated with only one scenario earthquake on a prototype bridge due to the scope limit. Therefore, some observations made above are only for this particular prototype bridge under the specific scenario seismic excitation, and more general conclusions can be made based on more systematic analyses of additional bridges and seismic inputs.

## 6. REFERENCES

- American Association of State Highway and Transportation Officials (AASHTO) (2012). LRFD bridge design specifications, Washington, D.C.
- Amzallag, C., Gerey, J. P., Robert, J. L., & Bahuaud, J. (1994). "Standardization of the rainflow counting method for fatigue analysis." *International Journal of Fatigue*, 16(4), 287-293.
- Billah, A. M., Alam, M. S., & Bhuiyan, M. R. (2012). "Fragility analysis of retrofitted multicolumn bridge bent subjected to near-fault and far-field ground motion." *Journal of Bridge Engineering*, 18(10), 992-1004.
- Blejwas, T. E., Feng, C. C., and Ayre, R. S. (1979). "Dynamic interaction of moving vehicles and structures." *J. Sound Vib.*, 67, 513–521.
- Caltrans, S. D. C. (2004). Caltrans Seismic Design Criteria version 1.3. California Department of Transportation, Sacramento, California.
- Chen, S. R., & Cai, C. S. (2007). "Equivalent wheel load approach for slender cable-stayed bridge fatigue assessment under traffic and wind: Feasibility study." *Journal of Bridge Engineering*, 12(6), 755-764.
- Chen, L., & Chen, S. (2016). "Seismic fragility performance of skewed and curved bridges in low-to-moderate seismic region." *Earthquakes and Structures*, 10(4), 789-810.
- Chen, S. R., and Wu, J. (2010). "Dynamic performance simulation of long-span bridge under combined loads of stochastic traffic and wind." *J. Bridge Eng.*, 10.1061/(ASCE) BE.1943-5592.0000078, 219–230.
- Chen, S. R. and Wu, J. (2011). "Modeling stochastic live load for long-span bridge based on microscopic traffic flow simulation." *Computer & Structures*, 89, 813-824.
- Chouw, N., & Hao, H. (2008). "Significance of SSI and nonuniform near-fault ground motions in bridge response I: Effect on response with conventional expansion joint." *Engineering Structures*, 30(1), 141-153.
- Choi, E., DesRoches, R., & Nielson, B. (2004). "Seismic fragility of typical bridges in moderate seismic zones." *Engineering Structures*, 26(2), 187-199.
- Deng, L., and Cai, C.S. (2010). "Development of dynamic impact factor for performance evaluation of existing multi-girder concrete bridges." *Engineering Structures*, 32(1), 21-31.
- Deng, L., Yu, Y., Zou, Q.L., and Cai, C.S. (2015). "State-of-the-art Review on Dynamic Impact Factors of Highway Bridges." *Journal of Bridge Engineering* (ASCE), 2015(5), 20(5), 04014080.
- DesRoches, R., & Muthukumar, S. (2002). "Effect of pounding and restrainers on seismic response of multiple-frame bridges." *Journal of Structural Engineering*, 128(7), 860-869.
- Fahmy, M. F., Wu, Z., Wu, G., & Sun, Z. (2010). "Post-yield stiffnesses and residual deformations of RC bridge columns reinforced with ordinary rebars and steel fiber composite bars." *Engineering Structures*, 32(9), 2969-2983

- Ghobarah, Ahamed (2001). "Performance-based design in earthquake engineering: state of development." *Engineering Structures*, 23, 878-884.
- Ghosh, J., Caprani, C. C., & Padgett, J. E. (2013). "Influence of traffic loading on the seismic reliability assessment of highway bridge structures." *Journal of Bridge Engineering*, 19(3), 04013009.
- Japan Road Association (2002). Design Specifications of Highway Bridges, Part V Seismic Design.
- Kameda, H, Murono, Y, Maekawa, Y, Sasaki N. (1992). "Dynamic structure-vehicle interaction for seismic load evaluation of highway bridges." In Proceedings of the Tenth World Conference on Earthquake Engineering.
- Kameshwar, S. and Padgett, J. (2017). "Effect of vehicle bridge interaction on seismic response and fragility of bridges." *Earthquake Engineering and Structural Dynamics*, 1-17.
- Kim, CW, Kawatani, M, Konaka, S, Kitaura, R. (2010). "Seismic responses of a highway viaduct considering vehicles of design live load as dynamic system during moderate earthquakes." *Struct Infrastruct Eng.* 2010;7(7–8):523-534.
- Kunnath SK, Erduran E, Chai YH, Yashinsky M. (2008). "Effect of near-fault vertical ground motions on seismic response of highway overcrossings. *Journal of Bridge Engineering*, 13(3):282–90.
- Maruyama Y. and Yamazaki, F. (2006). "Relationship between seismic intensity and drivers' reaction in the 2003 miyagiken-oki earthquake." *Structural Eng./Earthquake Eng.*, JSCE, 23 (1), 69-74.
- Mazzoni, S., McKenna, F., Scott, M. H., & Fenves, G. L. (2006). The Open System for Earthquake Engineering Simulation (OpenSEES) User Command-Language Manual.
- Muthukumar, S. (2003). A contact element approach with hysteresis damping for the analysis and design of pounding in bridges. Doctoral dissertation, Georgia Institute of Technology.
- Nielson, B. G. (2005). Analytical fragility curves for highway bridges in moderate seismic zones, Ph.D. Dissertation, Georgia Institute of Technology.
- Nikoukalam, M. T., & Sideris, P. (2016). "Low-Damage Posttensioned Segmental Bridge Columns with Flexible End Joints for Seismic Accelerated Bridge Construction." *Transportation Research Record: Journal of the Transportation Research Board*, (2592), 151-161.
- Newmark NM, Asce HM, Engrg C. "Seismic design spectra for nuclear power plants." *J Power Div, Am Soc Civil Eng* 1973;99:287–303. 99(P02).
- Padgett, J.E. and DesRoches, R. (2008), "Methodology for the development of analytical fragility curves for retrofitted bridges." *Earthq. Eng. Struct. Dyn.*, 37(8), 1157-1174.
- Shrestha, B., Hao, H., & Bi, K. (2013). "Pounding and unseating damage mitigation on bridge structures subjected to spatially varying ground motions using restrainers and rubber bumpers." Australian Earthquake Engineering Society Annual Conference, Tasmania, Nov. 15-17, 2013.
- Sivaramakrishnan, B. (2010). "Non-linear modeling parameters for reinforced concrete columns subjected to seismic loads." Doctoral dissertation, University of Texas.

Somerville, P. G. (2002). "Characterizing near fault ground motion for the design and evaluation of bridges." In Third National Conference and Workshop on Bridges and Highways. Portland, Oregon, April 2002.

Stanton, J.F. and McNiven, H.D. (1979). "The Development of a Mathematical Model to Predict the Flexural Response of Reinforced Concrete Beams to Cyclic Loads, Using System Identification." EERC Report Number 79/02, January 1979.

Tavares, D. H., Suescun, J. R., Paultre, P., & Padgett, J. E. (2013). "Seismic fragility of a highway bridge in Quebec." *Journal of Bridge Engineering*, 18(11), 1131-1139.

Timoshenko, S., Young, D. H., and Weaver, W. 1974. Vibration problems in engineering, 4th Ed., Wiley, New York.

Wibowo, H., Sanford, D. M., Buckle, I. G., & Sanders, D. H. (2012). "Effects of live load on seismic response of bridges: a preliminary study." *Civil Engineering Dimension*, 14(3), 166-172.

Wilson, T., Chen, S., & Mahmoud, H. (2015). "Analytical case study on the seismic performance of a curved and skewed reinforced concrete bridge under vertical ground motion." *Engineering Structures*, 100, 128-136.

Zhou, Y., and Chen, S. (2014). "Dynamic simulation of a long-span bridge-traffic system subjected to combined service and extreme loads." *Journal of Structural Engineering*, 141(9), 04014215.

Zhou, Y., and Chen, S. (2015). "Numerical investigation of cable breakage events on long-span cable-stayed bridges under stochastic traffic and wind." *Engineering Structures*, 105, 299-315.